

# Reliable estimation of the mean annual frequency of collapse by considering ground motion spectral shape effects

Alireza Azarbakht<sup>\*,1</sup>, Mohamadreza Shahri<sup>\*</sup> and Mehdi Mousavi<sup>\*</sup>

<sup>\*</sup> *Department of Civil Engineering, Faculty of Engineering, Arak University, Iran*

## ABSTRACT

Ground Motion Record (GMR) selection is an important issue in the Nonlinear Dynamic Analysis (NDA) procedure. Most of the current design codes recommend to use GMRs in which their mean spectrum be matched to a design spectrum e.g. uniform hazard spectrum. However recent research results have shown that the code methodology is neither robust nor realistic. On the other hand, GMR selection, based on spectral shape, is recently proposed in order to deal with this problem. Epsilon and Eta are two powerful spectral shape indicators which are used for GMR selection purposes. A comparison between Epsilon and Eta was made in order to access their capability to predict the linear spectral shape and the structural nonlinear response. The Eta-based Conditional Mean Spectrum (E-CMS), which has been recently emerged as a new design spectrum, was also investigated in this study. The E-CMS formulation format is fully compatible with the existing CMS definition which makes E-CMS quite easy to be implemented. The resulted E-CMS was used as a target spectrum for the record selection. Analysis of a set of Multi Degree Of Freedom (MDOF) systems shows that the mean annual frequency of collapse is achievable, with more reliability, based on the new emerged Eta indicator. Therefore, the bias is decreased by employing the Eta concept into the record selection procedure. The bias reduction is more significant in higher hazard levels and in the case of structures with low natural periods or with significant higher mode effects.

**KEY WORDS:** uniform hazard spectrum; Eta-based conditional mean spectrum; Epsilon indicator; Eta indicator; ground motion record selection; seismic hazard.

## 1. INTRODUCTION

The Pacific Earthquake Engineering Research (PEER) centre framework is a popular methodology in order to estimate the Mean Annual Frequency (MAF) of exceedance a particular Limit State (LS) [1] as expressed mathematically in Equation (1) [2].

$$MAF(LS) = \int \int_{IM, EDP} G(LS|EDP) \cdot |dG(EDP|IM)| \cdot |d\lambda(IM)| \quad (1)$$

where EDP is the engineering demand parameter, e.g. maximum inter story drift ratio;  $IM$  is the intensity measure, e.g. Spectral acceleration ( $Sa$ ) at the first period of a given structure and a damping ratio;  $G(LS|EDP)$  denotes the probability of exceeding LS conditioned on a specific value of EDP and  $G(EDP|IM)$  denotes the probability of exceeding EDP conditioned on a specific value of  $IM$ . One of the key points, in the calculation of Equation (1) is the inherent assumption about the dependence of EDP only on the chosen  $IM$ . If there is a dependence of EDP on any other indicator, except the chosen  $IM$ , then, Equation (1) results in a biased estimation of the discussed MAF. Hence, the sufficient  $IM$  is the  $IM$  which can represent the EDP without any dependence on other  $IM$  measures. The spectral acceleration at the first period of structure,  $Sa(T_1)$ , has been commonly used as the chosen  $IM$  in most of the former researches [3]. Most of the design codes use a suitable  $Sa$ -based target spectrum in order to facilitate ground motion record selection approaches and finally use those Ground

<sup>1</sup> Correspondence to: Alireza Azarbakht, Department of Civil Engineering, Faculty of Engineering, Arak University, Iran, P.O. Box 38156-88359. E-mail: [a-azarbakht@araku.ac.ir](mailto:a-azarbakht@araku.ac.ir)

Motion Records (GMRs) as input to dynamic analysis [4]. Uniform Hazard Spectrum (UHS) is commonly considered as the target in the most of design codes and guidelines [4]. This spectrum can be obtained by performing Probabilistic Seismic Hazard Analysis (PSHA [5]) calculations for spectral accelerations at a range of periods. Then, for a given rate of exceedance (e.g. 2% in 50 years) and for each period, the spectral acceleration amplitude, corresponding to that rate, is extracted. Those spectral acceleration values are then plotted versus periods, which result in UHS target spectrum. As every ordinate of the obtained target spectrum has an equal rate of being exceeded, this target is so-called a uniform hazard spectrum. It is worth mentioning that all ordinates are results of different earthquake events. As seen in Figure (1), comparison of UHS with an arbitrary recorded ground motion reveals that why UHS is not a realistic target spectrum. This fact is illustrated in Figure (1) which shows the UHS for 2% probability of exceedance in 50 years (2475 years return period) obtained by using the Campbell and Bozorgnia 2008 (CB08) attenuation prediction model [6] versus an example ground motion (Northridge event) and considering the target period equal to one second. The example spectrum is selected so that its  $Sa$  value at the period of one second be close enough to the  $Sa$  value of UHS. Significant differences are observed between the selected record spectrum and UHS in periods other than one second. Therefore, the uniform hazard spectrum, which is defined as the envelope of ground motions from many earthquakes, cannot be accounted as a good representative of a real single event. Many researchers have demonstrated that using UHS, as a target spectrum, results in highly conservative (over-prediction) of structural response under extreme ground motions [7-9]. Therefore, obtaining an accurate prediction of structural response is an important concern in recent years.

In addition to  $Sa$ -based elastic spectrum, many other approaches have been emerged to predict the response of a structure more accurately. It has been proved that  $Sa(T_1)$  is not sufficient enough especially when applied to the tall, long-period buildings [10], the structures with high levels of nonlinearity and in the near source regions [11, 12]. A more sufficient  $IM$  is less dependent on the seismic parameters, mainly magnitude and distance and Epsilon. To deal with this problem, some researchers tried to introduce new  $IMs$  which are more sufficient than the conventional  $Sa(T_1)$  [13]. Despite the  $IM$  sufficiency, the attenuation model availability plays an important role in this issue which makes many of the new proposed  $IMs$  inapplicable. Another approach is to use the conventional  $Sa(T_1)$  with additional criteria to avoid the bias when using Equation (1). For example, it is shown that the records, which have approximately the same Epsilon [9], can be employed with the conventional  $Sa(T_1)$  to increase the  $IM$  sufficiency [14] (Epsilon is described in the next section). This advantage was also employed in order to propose a new design spectrum which is called Conditional Mean Spectrum (CMS) [15]. CMS, which has been recently introduced to increase the  $Sa(T_1)$  sufficiency and decrease the UHS disadvantages, uses the advantages of the Epsilon as a spectral shape indicator [9]. The main assumption in the CMS calculation, for a single scenario earthquake, is that the spectral acceleration value at the target period (which is usually the natural period of the considered structure) is identical to the UHS spectral ordinate. Therefore, CMS has a peak at the target period and decays towards the median spectrum in other periods based on a correlation model.

As it is discussed before, the spectral acceleration is the only intensity measure which was employed in the development of CMS and the effect of other  $IMs$  are ignored. An alternative indicator, as a more reliable predictor of nonlinear response of structures, was proposed in [16] and named Eta. In the proposed study, it was shown that a simple linear combination of intensity measure Epsilons results in more robust prediction of nonlinear structural response as well as the spectral shape effects. In addition to the spectral acceleration, the Peak Ground Velocity (PGV) was also employed in the prediction of new spectral shape indicator [16]. A

new emerged target conditional mean spectrum was used in this paper which uses the Eta advantages instead of the conventional Epsilon [17]. The Eta-based Conditional Mean Spectrum (E-CMS) provides the mean response spectrum conditioned on the occurrence of a target spectral acceleration value at the period of interest with consideration of Eta-based correlation model. It is worth emphasizing that the corresponding developed formulation format is fully compatible with the existing CMS definition which makes the E-CMS quite easy to be implemented.

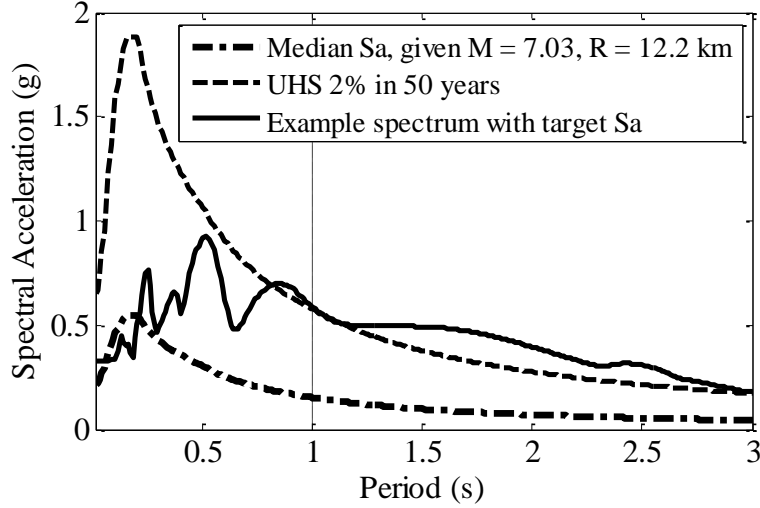


Figure 1: Median predicted spectrum, UHS for 2 % probability of exceedance in 50 years and the example spectrum which is the Newhall-W Pico Canyon Rd with  $M=6.7$  recorded from Northridge event [18].

## 2. A REVIEW ON EPSILON AND ETA AS PREDICTORS OF LINEAR SPECTRAL SHAPE

Recent studies have shown that the spectral shape has an important effect on the response of higher modes of structures as well as on its nonlinear behaviour [19]. For a given intensity measure, the Epsilon indicator measures the deviation of a given  $IM$ , for a recorded ground motion, from the  $IM$  computed from a Ground Motion Prediction Equation (GMPE). In other words, Epsilon is the difference between the natural logarithms of the two  $IMs$  normalized by the standard deviation of  $IM$  obtained from the chosen GMPE. This introduction to Epsilon indicator results in values having zero mean and unit standard deviation. The Epsilon indicator can be formulated in the mathematical form as written in Equation (2).

$$\varepsilon_{IM} = \frac{\ln(IM) - \mu_{\ln(IM)}}{\sigma_{\ln(IM)}} \quad (2)$$

where  $IM$  is the intensity measure for a given record;  $\sigma_{\ln(IM)}$  and  $\mu_{\ln(IM)}$  are, respectively, the mean and standard deviation of the intensity measure obtained from a specific GMPE (e.g. [6, 20]). The discussed intensity measure is (pseudo) spectral acceleration at the natural period of a given structure and damping ratio i.e.  $Sa(T_1, 5\%)$ .  $Sa(T_1, 5\%)$  was used because the majority of hazard curves are available in terms of spectral acceleration as a result of PSHA from well-known ground motion databases (e.g. United States Geological Survey). GMPEs, which provide ground motion intensity measures, such as peak ground acceleration or response

spectra as a function of magnitude and distance, are essential parts in the analysis of seismic hazard. These equations are typically developed using regressions over recorded GMR amplitude versus magnitude, distance and other seismic parameters.

Baker and Cornell have shown the importance of Epsilon as a spectral shape indicator [9]. They concluded that selected records with same  $Sa$  values at the target period, but different Epsilon values, result in different inelastic structural response. This fact is because Epsilon works as a proxy over average spectral shape. Therefore, the average spectral shape for negative and positive Epsilon values is different. Thus, the Epsilon indicator is taken as the robust predictor of spectral shape and not being influenced by the record linear scaling procedure [14]. As a result, the selection of GMRs, which are compatible with the target Epsilon, is a reasonable approach to increase the sufficiency of spectral acceleration [14]. The target Epsilon, for a given site, is calculated from a standard disaggregation analysis [21]. The obtained target Epsilon specifies the objective level of hazard and consequently corresponds to a particular spectral shape. Therefore, these summarized advantages are enough to identify Epsilon as an applicable indicator in order to select ground motions.

As Epsilon uses only one intensity measure, it was investigated more precisely and an alternative indicator of spectral shape, named Eta, was proposed. This new indicator leads to better prediction of the linear spectral shape as well as the nonlinear structural response [16]. The concept of the new spectral shape indicator was formed based on employing more  $IMs$  associated with  $Sa$ . The new spectral shape indicator was derived in order to increase the correlation between the Eta indicator with the nonlinear response of Single Degree Of Freedom (SDOF) structures. Eta was defined as a linear combination of  $IM$  Epsilons composed of the peak ground motions and spectral ordinates. The coefficients of  $IM$  Epsilons were determined through an optimization problem using Genetic Algorithm (GA) [22] so that the average correlation between the indicator and the nonlinear response of 84 SDOF systems with different periods and ductility became maximized. The Eta indicator improved the average correlation with the collapse capacity by approximately 50 percent. Therefore, the Eta can be accounted as a better predictor of structural nonlinear response instead of the conventional Epsilon. It was seen that a combination of PGV and  $Sa$  Epsilons results in the same correlation as employing all  $IM$  Epsilons. The Eta indicator can be expressed as written in Equation (3).

$$\eta(T) = 0.472 + 2.730\varepsilon_{Sa(T)} - 2.247\varepsilon_{PGV} \quad (3)$$

where  $\varepsilon_{Sa}$  and  $\varepsilon_{PGV}$  are, respectively, the observed spectral acceleration Epsilon and the peak ground velocity Epsilon which can be obtained by using Equation (2) and replacing  $IM$  by  $Sa$  and PGV. To clarify, 267 GMR horizontal components were employed as described in [19]. The mean spectra based on  $N$  records, which have the highest/lowest Epsilon values and the highest/lowest Eta values, are shown in Figure (2) and compared with the mean spectrum based on all GMRs. Both of Epsilon and Eta are obviously, as seen in Figure (2), spectral shape indicators. However, the difference between the mean spectral shape based on  $N=8$  and  $N=50$  is not significant in the case of Eta, as seen in Figure (2b) and (2d), whereas it is meaningful in the case of Epsilon as seen in Figure (2a) and (2c). In other words, Eta can predict the spectral shape with less numbers of GMRs which means that it is a better indicator of spectral shape effects in comparison with the conventional Epsilon in the record selection process.

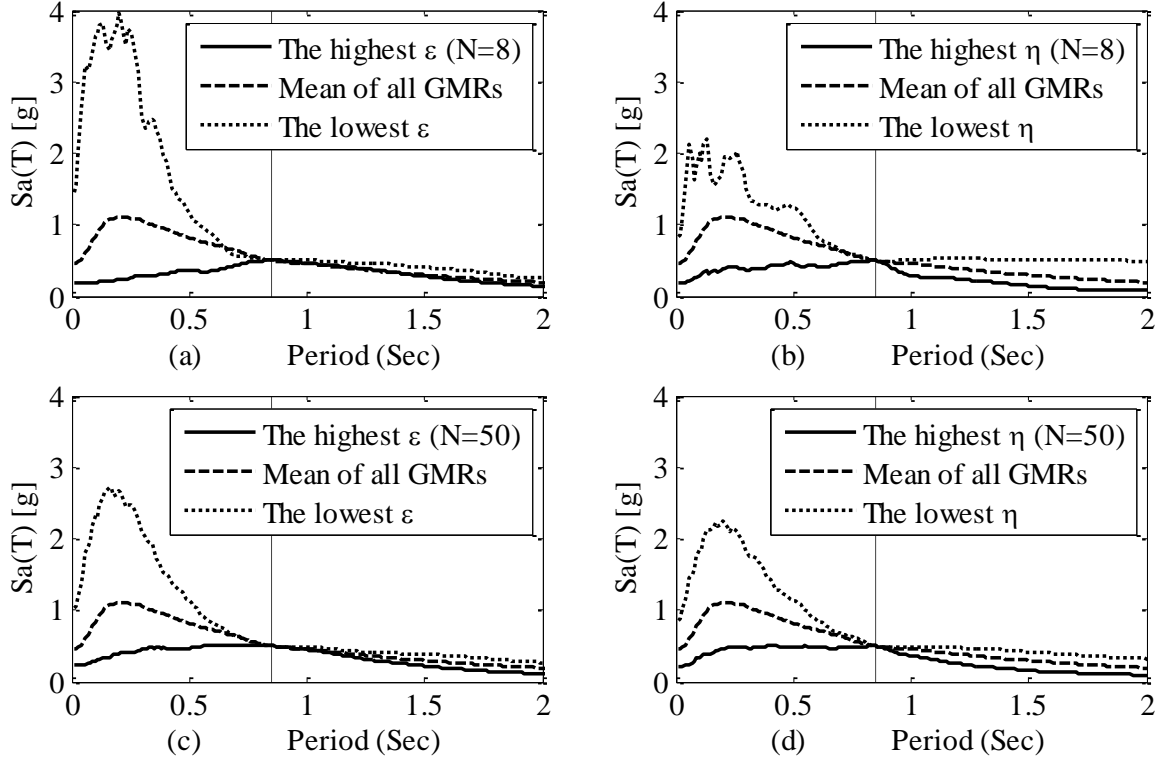


Figure 2: Comparison of the mean spectrum based on 534 GMRs with (a) the mean spectrum based on  $N=8$  highest/lowest Epsilon, (b) the mean spectrum based on  $N=8$  highest/lowest Eta (c) the mean spectrum based on  $N=50$  highest/lowest Epsilon, (d) the mean spectrum based on  $N=50$  highest/lowest Eta.

Note that  $\varepsilon_{PGV}$  is not a function of period and is constant over all spectral values. This characteristic allows us to arrange a closed form formula for the E-CMS in the following sections. Also note that the old GMPEs only provide predicted  $S_a$  and the corresponding logarithmic standard deviation (e.g. [23, 24]). Therefore, employing a suitable GMPE is an essential part in our study. For this purpose, CB08 GMPE was used since Eta has been obtained based on this model [16] in addition to the ability of PGV prediction. The CB08 model has used a subset of the PEER NGA database, and excluded recordings that were believed to be inappropriate for estimating free-field ground motions from shallow crustal earthquake main shocks in active tectonic regimes. Also note that, the Eta equation was derived in such a way to have the same value as the target Epsilon that can be achieved by hazard disaggregation analysis [16]. The same target Eta (equal to the target Epsilon) is used in Equation (3) in order to calculate the Eta value for each ground motion record.

### 3. INFLUENCE OF EPSILON AND ETA ON THE NONLINEAR SEISMIC RESPONSE OF STRUCTURES

The influence of Epsilon and Eta on linear spectral shape has been discussed in the previous section. However, their influence on the nonlinear response of structures is still an important issue which needs to be investigated. The spectral shape characteristics are especially important for the structural collapse assessment since the difference between the shape of UHS and the median predicted spectrum for a causal event is most significant in the range of high amplitudes [17]. Therefore, when assessing a probability of collapse under high amplitude motions, the choice of ground motions significantly impacts the collapse

assessment [25]. In addition, it was shown that Epsilon has a high correlation with the structural damage capacity values [25].

The capability of Epsilon, in prediction of nonlinear response of SDOF and Multi Degree Of Freedom (MDOF) structures, has been proved before [26]. The correlation of the spectral shape indicator with the nonlinear response of structures (collapse in this case) is considered in this study as the robustness of a given spectral shape indicator. For this purpose, a 12 storeyed concrete moment frame system with the first period of vibration equal to 2 sec was assumed. The structure is defined as ID 1019 in reference [26] in which more details are available. A set of 78 ground motion records, which was also employed by other researchers [26] is used here. All records were selected as input to dynamic analysis of the structure and they were scaled up to obtain the collapse of the structure by means of Incremental Dynamic Analysis (IDA) [27]. Figure (3) shows the collapse values of the given structure corresponding to 78 records versus their Epsilon and Eta values. As it was expected, both indicators have high correlations with the nonlinear collapse response. However, the Eta indicator shows higher correlation which indicates that it can be accounted as a better predictor of nonlinear response in comparison with the conventional Epsilon. It was shown that for two GMRs, with similar  $\varepsilon_{Sa}$ , the record with the higher  $\varepsilon_{PGV}$  (which corresponds to the lower Eta value) is expected to result in the lower collapse capacity and vice versa [16]. Additionally, the previous findings have demonstrated that the PGA/PGV ratio is related to the frequency content of GMRs (PGA denotes peak ground acceleration) [28, 29]. Therefore, it is expected that a rational combination of spectral ordinates with PGV indicator can express the structural response more appropriately. However, this issue is of great interest for future researches.

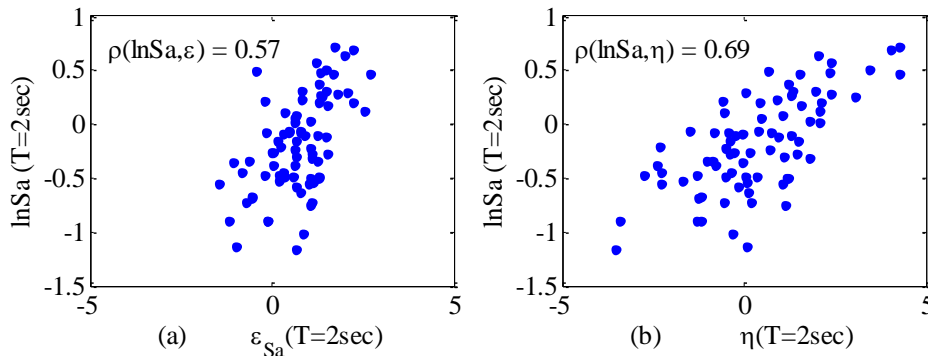


Figure 3: Correlation between collapse pseudo acceleration of MDOF structure (ID 1019) for all 78 records with: (a) in the case of Epsilon, (b) in the case of Eta.

Now suppose that the aim is to filter a specified number of records to account for a given seismic hazard level. The considered hazard level was chosen as two percent probability of exceedance in 50 years (2475 year return period). Disaggregation analysis, as a result of PSHA, provides information about the earthquake scenario (such as mean casual Epsilon that is the target Epsilon value) which causes the desirable hazard. The target Epsilon, at the period of two seconds, was considered here to be equal to two. This assumption is obtained by U.S. Geological Survey (USGS) disaggregation tool based on a site in Riverside, California (latitude/ longitude = 33.979/-117.335) [30]. The aim is to select ground motion records in order to evaluate the mean value of structural collapse. Therefore, 20 records, out of 78 records, were filtered in which they had Epsilon values closest to the target Epsilon value at the period of 2 sec. The mentioned approach is also repeated for Eta indicator. It is worth emphasizing that the target Eta is equal to the target Epsilon as the Eta indicator has been

normalized in Equation (3). The correlation between the collapse values of the filtered records and their Epsilon and Eta values was computed as well. The results are shown in Figure (4). As it was expected, the correlation obtained by employing the Eta indicator is still higher than the associated correlation with the conventional Epsilon. In fact, it is concluded that the higher correlation represents meaningful relationship between the Eta and nonlinear collapse response. To prove this hypothesis, a statistical test was also used in order to investigate the accuracy of the results. The P-value was defined as the likelihood of observing a correlation coefficient equal to or greater than  $\rho$  if the value of  $\rho$  is in fact zero. Lower P-value means that the record filtration without caring at Epsilon/Eta indicator is not a good strategy. Therefore the Epsilon and Eta have statistically significant effects on the structural response.

The lower P-value for the Eta filtration approach (e.g. less than 5% significance level), as seen in Figure (4b), indicates the significance of the correlation coefficient. Therefore, it is claimed that the Eta indicator is the more powerful predictor of nonlinear response when compared with the Epsilon, at least in the case of the considered MDOF structure. The main concern may still be the validation of the results since the justification is only based on one MDOF system. To validate the results, a set of different MDOF systems, with various properties, were taken into consideration and the filtration approach was repeated again. More details about the structures can be found in [26].

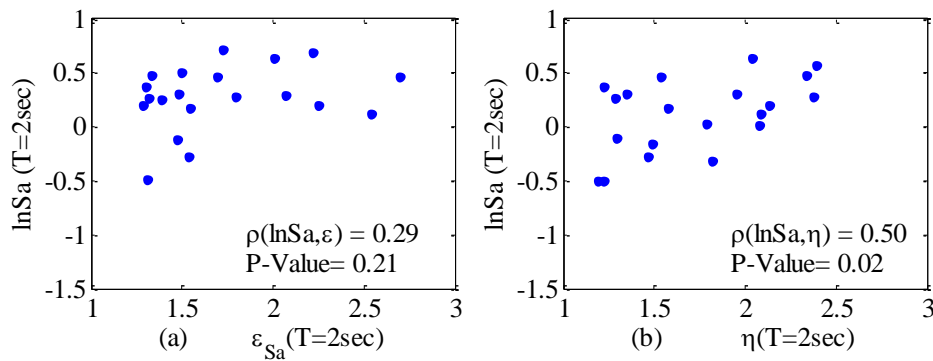


Figure 4: Correlation between collapse pseudo acceleration of MDOF structure (ID 1019) for 20 filtered records with (a) in the case of Epsilon, (b) in the case of Eta.

The results are summarized in Table (1). As seen in the nonlinear correlation column in Table (1), both indicators have high correlations with the nonlinear collapse response. However, the correlation value in the case of Eta indicator is higher. In the last three columns in Table (1), the mean values, corresponding to the structural collapse, are compared in the cases of Epsilon filtration, Eta filtration and no filtration approaches. As a consequence of higher correlation coefficients in the case of Eta filtration, when compared with the Epsilon filtration and no filtration approaches, it is claimed that the structural collapse is more reliable when the Eta filtration approach is employed.

Note that the structure with ID 1019 is the assumed structure which was investigated in details in Figure (3) and (4). All of the discussed structures will also be used in further sections.

Table 1: Comparing Epsilon and Eta in prediction of nonlinear response by filtering 20 records, and mean of collapse.

ID	No. of stories	$T_1$ [sec]	Nonlinear correlation			Mean of collapse	
			$\rho(\ln Sa, \varepsilon)$	$\rho(\ln Sa, \eta)$	$\varepsilon$ filtration	$\eta$ filtration	All records
2061	1	0.42	0.571	0.794	0.836	0.950	1.046
1001	2	0.63	0.519	0.709	1.046	1.004	1.134
1003	4	1.12	0.482	0.587	0.275	0.159	0.237
1019	12	2	0.566	0.690	0.274	0.117	-0.181
1020	20	2.63	0.504	0.672	-0.392	-0.450	-0.601

#### 4. ETA-BASED CONDITIONAL MEAN SPECTRUM

The Eta-based conditional mean spectrum is discussed in this section as a new emerged target spectrum for the record selection purposes [17]. First, it is needed to define a target spectral acceleration value at a period of interest. The period of interest is usually computed by modal analysis of a particular structure ( $T^*$ ). Usually the target period is chosen equal to the first mode period of vibration ( $T_1$ ). The mean causal magnitude ( $M$ ), mean causal distance ( $R$ ) and mean causal Epsilon ( $\varepsilon_{Sa(T^*)}$ ) were obtained by employing the disaggregation analysis (e.g. from [30]) based on the probabilistic seismic hazard analysis. The mean predicted spectral acceleration ( $\mu_{\ln Sa}$ ) and corresponding standard deviation of the logarithmic spectral acceleration ( $\sigma_{\ln Sa}$ ) were calculated using existing ground motion prediction models (i.e. CB08 in this paper [6]). The probability calculation shows that the Epsilon values ( $Sa$ -based) at other periods are equal to the target Epsilon value multiplied by the correlation coefficient between the two Epsilon values as written in Equation (4) [15]. Consequently, the CMS value at the target period is calculated simply by rearranging Equation (2) which is written in Equation (5) [15].

$$\varepsilon_{Sa(T)} = \rho_{\varepsilon(T), \varepsilon(T^*)} \varepsilon_{Sa(T^*)} \quad (4)$$

$$Sa(T) = \exp(\mu_{\ln Sa(T)} + \sigma_{\ln Sa(T)} \varepsilon_{Sa(T)}) = \exp(\mu_{\ln Sa(T)} + \sigma_{\ln Sa(T)} \rho_{\varepsilon(T), \varepsilon(T^*)} \varepsilon_{Sa(T^*)}) \quad (5)$$

The correlation coefficient can be obtained by Bakers prediction equation as a close form solution [31, 32] or using the correlation based on a suitable subset of GMRs (e.g. from NGA database). The GMRs which were used in this study can be found in reference [19].

The target Epsilon and target Eta are needed for E-CMS calculation. However, the disaggregation analysis only provides the target Epsilon. Therefore, the Eta equation is normalized to the target Epsilon value in Equation (3) [16]. The target Eta can now be considered to be equal to the target Epsilon which is one of the disaggregation results ( $\eta^* = \varepsilon_{Sa(T^*)}$ ). The target peak ground velocity ( $\varepsilon_{PGV}$ ) is achievable as written in Equation (6), by using Equation (3), and considering the equality of the target Epsilon ( $\varepsilon_{Sa(T^*)}$ ) with the target Eta ( $\eta^*$ ).

$$\varepsilon_{PGV} = \frac{1}{2.247} (0.472 + 1.730 \varepsilon_{Sa(T^*)}) \quad (6)$$

Again note that the peak ground velocity Epsilon is a period independent parameter and is constant over the whole period range. Substitution of Equation (2) and (6) into Equation (3), produces the conditional mean spectrum based on Eta indicator as written in Equation (7). The Eta values at other periods are predicted by using the correlation approach according to Equation (4) by replacing  $\eta$  instead of  $\varepsilon$  i.e.  $\eta(T) = \rho_{\eta(T), \eta(T^*)} \eta(T^*)$ .

$$Sa(T) = \exp(\mu_{\ln Sa(T)} + \frac{\eta^* \sigma_{\ln Sa(T)} (\rho_{(\eta(T), \eta(T^*))} + 1.730)}{2.730}) \quad (7)$$

where  $\rho_{(\eta(T), \eta(T^*))}$  is the correlation coefficient between Eta in an arbitrary period ( $T$ ) and the target period ( $T^*$ ). It is obvious that Eta, in an arbitrary period ( $T$ ), is equal to the Eta in the target period multiply by the correlation coefficient between the two corresponding Eta values. This correlation coefficient is discussed in Appendix A. It is also clear that the target  $Sa$  value in E-CMS is equal to the CMS value at the target period i.e. replacing  $\rho$  value by one. In other words, both Epsilon and Eta-based spectra are conditioned on  $T^*$ . It is worth noting that the general similarity between Equation (5) and (7) allows the final simple formulation for E-CMS which is quite similar to the conventional CMS formulation. This issue is discussed in the following section.

#### 4.1. Example: deriving E-CMS spectrum

A simple structure with a first-mode period of 1 second and 5% critical damping ratio was assumed, and 2% probability in 50 years was considered as a given hazard level. The shear wave velocity and other seismic parameters are given as:

- Shear wave velocity = 760 (m/s).
- Depth to the top of co-seismic rupture = 0 (km).
- Rake angle = 35 (degree).
- Dip = 90 (degree).
- Depth to the 2.5 km/s shear wave velocity horizon = 2.5 (km).

The median predicted spectral acceleration is equal to 0.17g and the standard deviation is equal to 0.66 in the target period (1sec) in which both were obtained by using CB08 GMPE. The mean causal values from the disaggregation analysis are required. Therefore, the following mean values were assumed for an ideal site:

- Mean causal magnitude: 7.0
- Mean causal distance: 10 km
- Mean causal Epsilon: 1.4

As the obtained Epsilon from the disaggregation analysis is assumed to be equal to the target Epsilon, the other Epsilon values at other periods can be determined as well. For this purpose, a linear regression (a correlation model) is needed to be employed. Baker and Jayaram proposed a model for the correlation coefficient calculation between two Epsilon values based on the Chiou and Youngs GMPE [33]. This method is consistent enough with other GMPEs with high level of accuracy. Epsilon values, Eta values and the correlation coefficients were computed in this study based on the considered GMR database without using any closed-form solution. Figure (5) shows a contour of the correlation coefficient between two arbitrary Epsilon and Eta values respectively. The period range was taken between 0.01 to 5 sec. Finally, the Epsilon-based conditional mean spectrum was computed by Equation (5) and the Eta-based conditional mean spectrum was obtained by using Equation (7). Figure (6) compares the CMS, E-CMS, median and UHS spectra for the given simple example. In the long period values, which is an essential part in the nonlinear response of structure, as seen in Figure (6), CMS and E-CMS are matched well. Therefore, the nonlinear response seems to be as effective as both CMS and E-CMS are able to produce. However, a noticeable difference between CMS and E-CMS is apparent in the low period range which influences the higher

modes of structures. In other words, the multi degree of freedom structures as well as stiff SDOF systems are good candidates to be employed for investigation of the discussed difference. Both CMS and E-CMS have a peak at the period of one second since the correlation coefficient is equal to unity at the target period. The correlation coefficients decrease at large and small periods but the reduction process is more rapid in the CMS case in comparison with the E-CMS case. In other words, E-CMS values in smaller periods are larger than the CMS values. This fact can be investigated if Equation (7) be rearranged to produce Equation (8) by using Equation (9). Equation (8) is a simple formulation for E-CMS which is quite similar to the conventional CMS formulation (Equation 5).

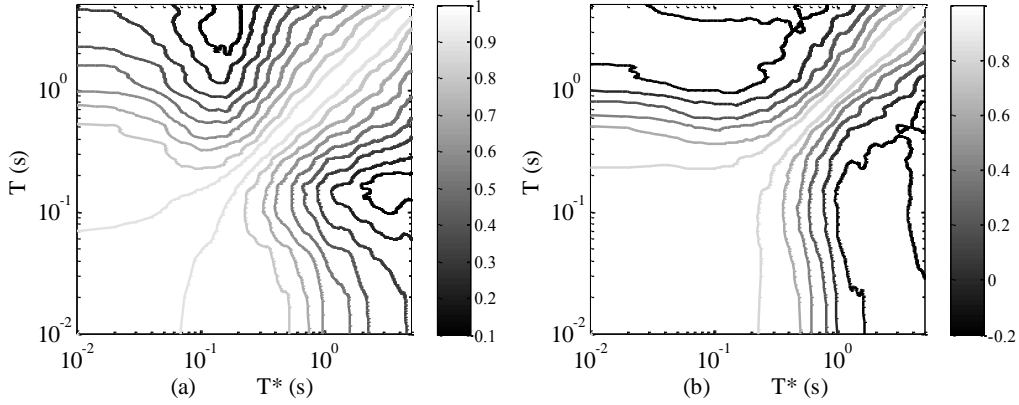


Figure 5: Empirical correlation coefficients based on the considered GMR database. (a) For Epsilon. (b) For Eta. ( $T$ : Period of interest,  $T^*$ : Target period)

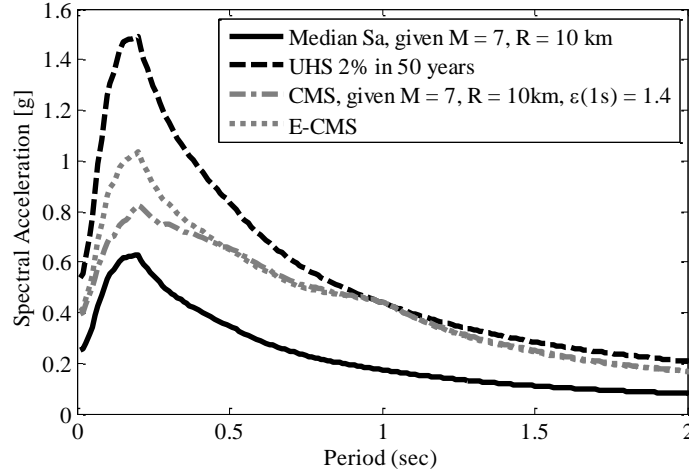


Figure 6: UHS, Epsilon-based and Eta-based conditional mean spectrum for an ideal site, given  $M=7$ ,  $R=10$  km,  $\epsilon=1.4$ .

$$S_a(T) = \exp(\mu_{\ln S_a(T)} + \eta^* \sigma_{\ln S_a(T)} \rho'_{(\eta(T), \eta(T^*))}) \quad (8)$$

where  $\rho'$  can be defined as:

$$\rho'_{(\eta(T), \eta(T^*))} = \frac{\rho_{(\eta(T), \eta(T^*))} + 1.73}{2.730} \quad (9)$$

By comparing Equation (8) with Equation (5), it is revealed that the only difference between the predicted  $Sa$  values is the correlation coefficient. In other words, the source of difference between CMS and E-CMS is just the correlation coefficient.

This fact is also shown in Figure (7) where the parameter  $\rho'$  for Eta and  $\rho$  for both Epsilon and Eta are compared. Note that, Figure (7) explains the correlation values, and do not reflect the spectral acceleration terms. However, this figure justifies the differences between the CMS and E-CMS spectra since CMS is based on  $\rho$  and E-CMS is based on  $\rho'$ . Figure (6) shows that the difference between the two spectra begins from the approximate period of 0.5 sec to lower periods where this difference is also presented in Figure (7). It can be seen in Figure (7) that the Eta correlation values are lower than the Epsilon correlation values. The lower period bound is related to the response of higher modes of vibration. As an important result, the CMS underestimates  $Sa$  values against E-CMS for short period structures as well as the medium period structures with strong higher modes effects.

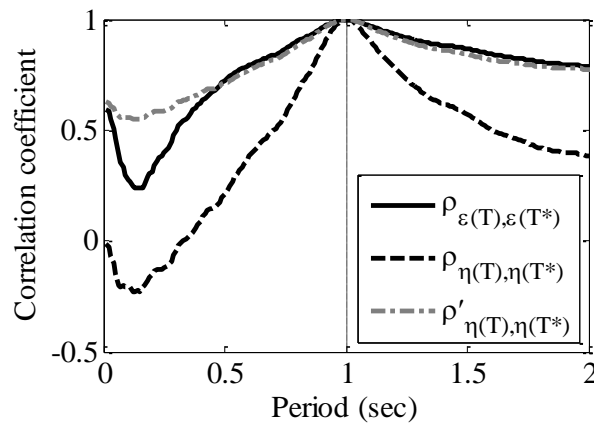


Figure 7: The correlation coefficients over a period range.

As the correlation between Eta and structural response is higher than the corresponding correlation between Epsilon and structural response [16], it can be tentatively claimed that E-CMS is more realistic spectrum than the conventional CMS spectrum. The target period was taken to be equal to the first-mode period of vibration. This assumption is not necessarily reliable, because the sensitivity of the results versus the considered structure is not discussed yet. Therefore, an effort should be done in order to find the critical target period. Accordingly, the record selection can be repeated by different CMS or E-CMS. Separate sets of selected records, based on different CMS or E-CMS, can be used for analysis and the effect of choosing the target period can be investigated more precisely. Finally, it can be inferred that which target period is more sensitive, and it can be chosen as an appropriate target period. Figure (8) shows two E-CMS cases computed by different target periods and this issue is left for future research.

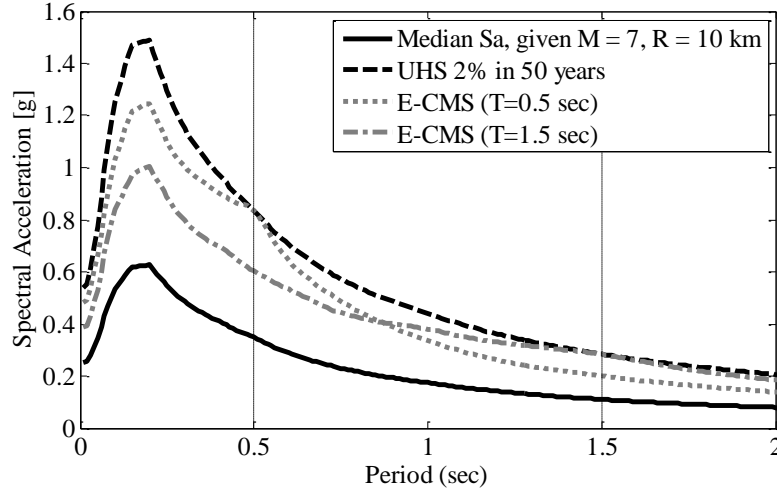


Figure 8: Eta-based conditional mean spectra in different periods for an equal probability of exceedance 2% in 50 years. ( $T^*=0.5$  sec &  $T^*=1.5$  sec).

## 5. MEAN ANNUAL FREQUENCY OF COLLAPSE FOR TEST STRUCTURES BY USING EPSILON AND ETA FILTRATION APPROACHES

An eight-storeyed reinforced concrete structure, as a test structure, is investigated in this section. The building is  $36.5 \times 36.5$  m in plan, uses a 3-bay perimeter frame system with a spacing of 6.1 m, and has a fundamental period ( $T_1$ ) equal to 1.71 second designed based on modern building codes. This building is ID 1011 in [26]. A simple seismic scenario was chosen as seen in Figure (9). The only seismic potential is located in 11 km from the site with the possibility of producing an earthquake with the moment magnitude equal to 7.2 in every 200 years. The 30 m soil shear wave velocity was assumed to be 360 m/s. The corresponding hazard curve is shown in Figure (9) and the target Epsilon values for different hazard levels are summarized in Table (2). As an example, in the case of 200 years return period, which is equal to 22% probability of exceedance in 50 years, the mean and standard deviation of spectral acceleration are calculated by using CB08 GMPE which are, respectively, equal to 0.2128 and 0.676. The spectral acceleration, corresponding to the 200 years return period, is equal to 0.0098 based on the hazard curve in Figure (9). Therefore, the target Epsilon is simply calculated as written in Equation (10).

$$\varepsilon_{Sa}^* = \frac{\ln(Sa) - \mu_{\ln(Sa)}}{\sigma_{\ln(Sa)}} = \frac{\ln(0.0098) - \ln(0.2128)}{0.676} \approx -4.56 \quad (10)$$

A set of 78 real ground motion records was employed in this section which previously used in Section 3. A set of 20 records was used for the analysis in each hazard level based on the target Epsilon. For example, the whole (78) records were sorted based on Epsilon corresponding to 22% probability of exceedance in 50 years. Then, 20 records were filtered in which their Epsilon values have the smallest difference with the target Epsilon which is -4.56 in this case. By considering the collapse data associated with the 20 records (here the limit state is supposed to be the Collapse Prevention (CP) [1] and indicated by non-convergence of dynamic analysis), the probability of collapse was calculated. This probability of collapse (which is interpreted as the collapse fragility curve) was computed from a parametric

distribution by fitting a lognormal distribution to the intensity levels of ground motions that cause the collapse of a structure as mathematically written in Equation (11).

$$P(\text{Collapse} | Sa_i) = \Phi\left(\frac{\ln(Sa_i) - \mu}{\sigma}\right) \quad (11)$$

where  $Sa_i$  is the spectral acceleration of interest,  $\mu$  and  $\sigma$  are the estimated mean and standard deviation of the collapse capacity in terms of  $Sa$  as an *IM*. The collapse, in terms of spectral acceleration in the four assumed considered hazard levels, was calculated based on nonlinear response history analysis. The results are given in Table (3) which confirm that the filtration based on Epsilon and Eta influences on the mean of collapse. The corresponding fragility curves are shown in Figure (10). The difference between the two fragility curves, based on Epsilon and Eta filtrations, as seen in Figure (10), is not negligible. For more clarification, the mean annual frequency of collapse was calculated for this test structure. It is worth mentioning that the MAF value should be calculated over a range of intensity measures. In other words different 20 records should be taken into account in each level of  $Sa$ . The results are shown in Figure (11a) and Table (4). As seen in Figure (11a), the MAF value based on the Eta filtration approach is quite smaller than the MAF based on the Epsilon filtration and no filtration approaches. The y axis is defined as the derivative of the MAF with respect to the  $Sa$ . Again, it is claimed that the MAF based on the Eta filtration approach is more realistic than the conventional Epsilon since the Eta is more correlated with the nonlinear structural response.

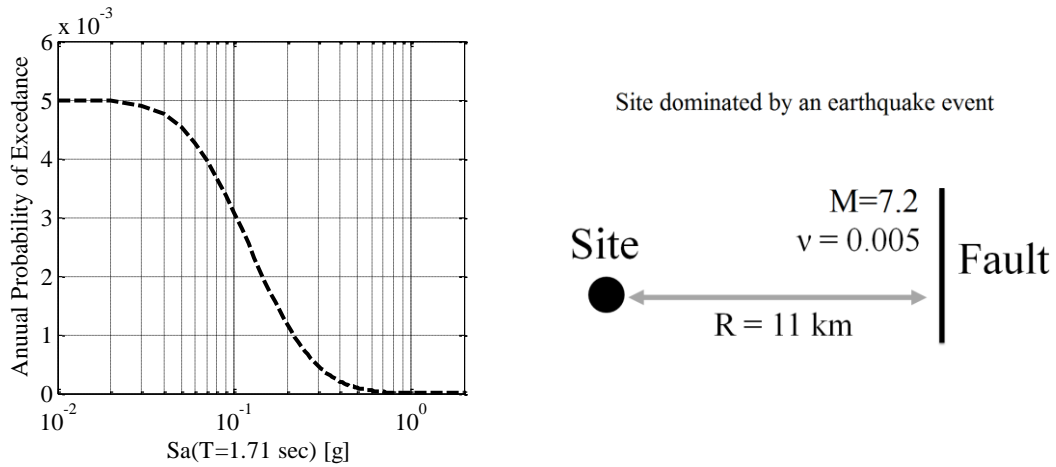


Figure 9: (left) the seismic hazard curve for the given scenario; (right) a schematic representation of the chosen seismic scenario.

Table 2: The target Epsilon values for different hazard levels.

Probability of exceedance in 50 years	Years Hazard level	Target Epsilon
22 %	200	-4.56
13 %	400	0.00
10 %	475	0.20
2 %	2475	1.40

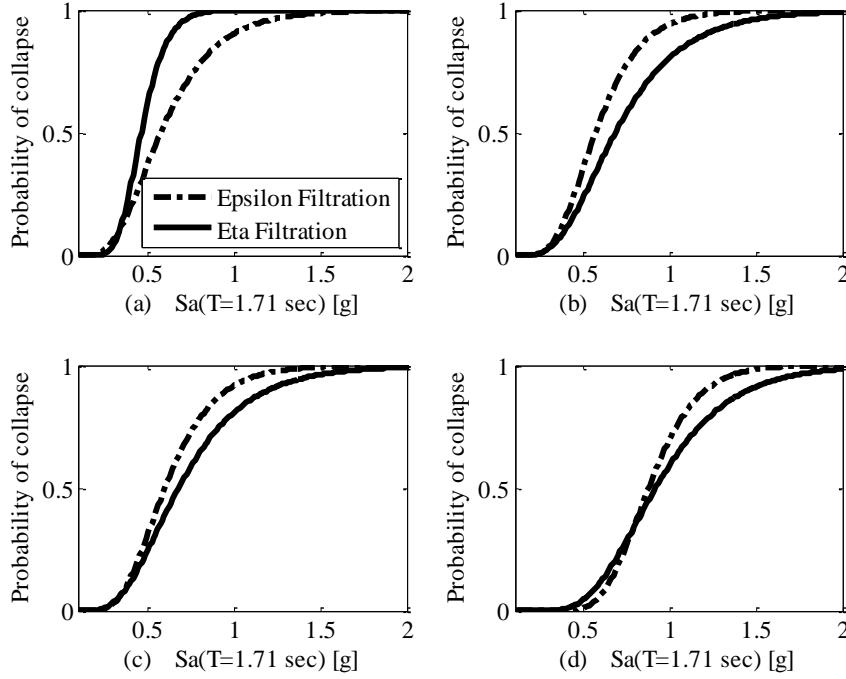


Figure 10: Fragility curves in four different hazard levels for two Epsilon and Eta filtration approaches; (a) 200 years; (b) 400 years; (c) 475 years; (d) 2475 years.

Table 3: The mean collapse in terms of spectral acceleration in four considered hazard levels.

Years hazard level	$\varepsilon$ Filtration	$\eta$ Filtration
200	0.627	0.472
400	0.604	0.743
475	0.636	0.738
2475	0.899	0.969

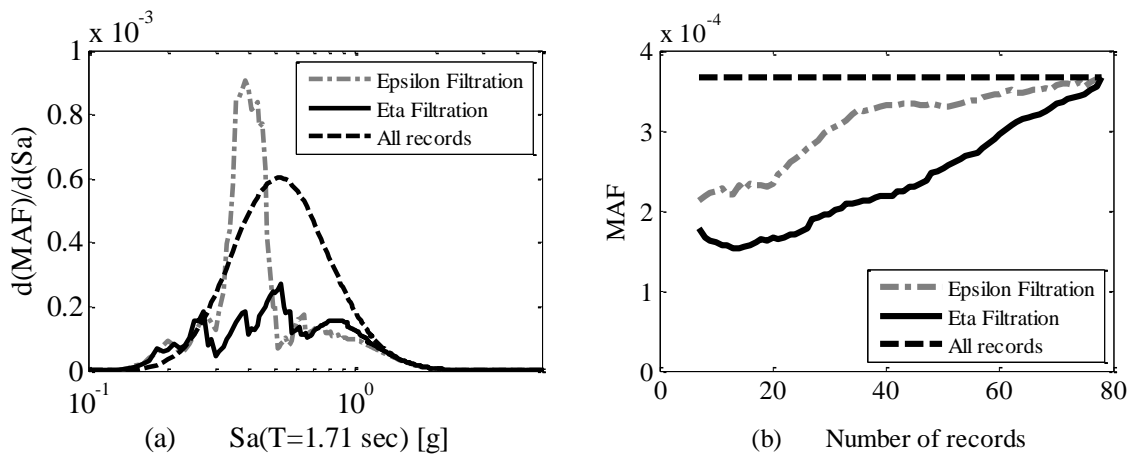


Figure 11: (a) The MAF for the considered eight story structure (ID 1011) with  $T=1.71$ s; (b) The MAF variation versus number of employed records for building ID 1011.

Table 4: The MAF for building ID1011 by different filtration approaches and using 20 records.

Filtration	MAF (*10 <sup>-4</sup> )
All records	3.66
$\epsilon$ Filtration	2.33
$\eta$ Filtration	1.65

The lower MAF value, which was obtained for the eight storeyed building, is not a universal conclusion for other structures. To clarify, a set of MDOF buildings was taken into account as shown in Table (5). All the considered buildings were designed based on ASCE 7-02 standard [26]. The fundamental period of the thirty buildings varies from 0.4s to 2.6s which is a wide range of interest. The former eight storeyed building is one of these selections with ID 1011. The correlation of Epsilon and Eta with the structural nonlinear response is also provided in Table (5). The results are meaningful in which all cases show more correlation in the case of Eta when compared with the Epsilon case.

The MAF results are shown in Table (5) for three different approaches including Eta filtration, Epsilon filtration and no filtration. In the majority of cases, the Eta filtration MAF is less than the Epsilon filtration MAF and both are less than the no filtration MAF. The sufficient number of records, which was used to calculate the MAF value, is still a question. The variation of MAF versus the number of considered records is shown in Figure (11b). A set of seven records was used for the start point which reflects the conventional number in the most guidelines and finally 78 records were selected. The starting section of the curve in Figure (11b) confirms that the Eta and Epsilon filtrations significantly change the MAF estimation. The difference between the Eta filtration and the Epsilon filtration varies for different buildings which can be assigned to the characteristics of each case.

## 6. COLLAPSE FRAGILITY CURVES BASED ON CMS AND E-CMS SPECTRA

The use of CMS and E-CMS, as target design spectra, is investigated in this section as shown in Figure (12). A set of 20 records, out of 534 records, was selected in which their mean spectrum matches to the target design spectrum (the target design spectra are CMS and E-CMS in Figure (13) and (14)). The genetic algorithm, as an efficient optimization method, was utilized to solve this optimization problem.

It is obvious that, the optimization problem has not a unique solution and it is more time consuming in comparison with the filtration approach. The hazard assumptions were also the same as the previous section. The given structure in this section was supposed to be the SPEAR building. The detail characteristics can be found in [34]. The SPEAR building is a 3-storeyed 3D reinforced concrete structure for which a pseudo-dynamic experiment was performed at full scale at the ELSA Laboratory, within the European research project SPEAR (“Seismic performance assessment and rehabilitation of existing buildings”) [34]. The structure has  $T_1=0.85$  sec. A more detailed explanation of the model and comparison of experimental and numerical results can be found in [35].

The response of the given structure was calculated by means of incremental dynamic analysis as seen in Figure (15). The specified points are corresponding to the global instability which have been interpreted to the collapse capacity in this paper. The cumulative distribution function of the capacity points, in terms of  $S_a$ , was calculated as seen in Figure (16) for 2475 years hazard level by employing Equation (11). It is obvious that the fragility curves are significantly influenced by the record selection approach. The mean collapse capacity, in terms of  $S_a$ , is also given in Table (6) for different record selection approaches. The mean

value is the arithmetic mean of collapse values obtained by 20 selected records. As it was expected, the mean value of structure response is increased when the records based on E-CMS has been employed. It means that, the CMS selection is non-conservative in this case. It is also worth mentioning that the difference between the two approaches increases for the higher levels of hazard as seen in Table (6).

Table 5: The thirty building characteristics and the corresponding MAF by 20 filtered records in three different approaches.

Design information and Period			Nonlinear Correlation			MAF (multiplied by $10^{-4}$ )			
ID	Stories	Framing System	$(T_I)$ [sec]	$\rho_{(\ln Sa, \epsilon)}$	$\rho_{(\ln Sa, \eta)}$	Epsilon Filtration	Eta Filtration	All records	
2061	1	Space	0.42	0.571	0.794	0.789	0.468	1.733	
2062			0.42	0.561	0.782	0.449	0.26	1.199	
2063			0.42	0.568	0.793	0.792	0.464	1.727	
2069			Perimeter	0.71	0.537	0.730	3.13	3.509	4.014
1001	2	Space	0.63	0.519	0.709	0.167	0.160	0.632	
1001a			0.56	0.444	0.696	0.279	0.297	0.627	
1002			0.63	0.465	0.688	0.467	0.491	1.071	
2064			Perimeter	0.66	0.529	0.720	1.056	1.126	2.054
1003	4	Perimeter	1.12	0.482	0.587	1.784	1.135	2.716	
1004			1.11	0.417	0.559	1.228	0.711	1.966	
1008			Space	0.94	0.524	0.550	0.755	0.954	1.493
1009			Perimeter	1.16	0.472	0.574	1.178	0.568	2.062
1010	8	Space	0.86	0.452	0.645	0.194	0.243	0.711	
1011			Perimeter	1.71	0.514	0.714	2.336	1.655	3.662
1012			1.8	0.535	0.674	0.822	0.686	1.946	
1022			1.8	0.512	0.588	0.516	0.569	1.425	
2065	12	Space	1.57	0.491	0.663	0.714	0.740	1.864	
2066			1.71	0.510	0.643	0.458	0.347	1.43	
1023			1.57	0.440	0.598	1.729	1.641	2.797	
1024			1.71	0.453	0.633	1.315	0.950	2.428	
1013	20	Perimeter	2.01	0.536	0.701	1.545	1.404	2.90	
1014			2.14	0.538	0.627	0.987	0.971	2.091	
1015			2.13	0.554	0.629	0.817	0.790	1.792	
2067			Space	1.92	0.475	0.645	0.726	0.696	1.756
2068	20	Space	2.09	0.561	0.619	0.817	0.864	1.943	
1017			1.92	0.449	0.518	1.484	1.684	2.552	
1018			2.09	0.520	0.582	1.105	1.145	2.336	
1019			Space	2	0.566	0.690	0.487	0.452	1.495
1020	20	Perimeter	2.63	0.504	0.672	0.92	0.532	1.451	
1021			Space	2.36	0.559	0.637	0.559	0.541	1.160

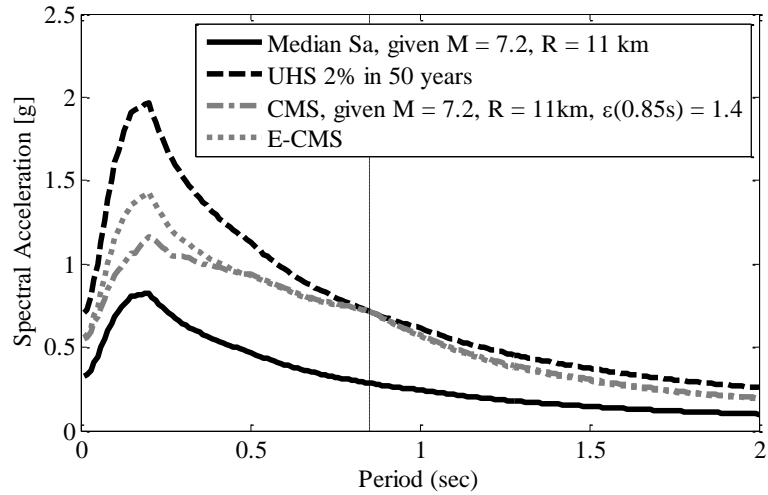


Figure 12: UHS, CMS, E-CMS and the median spectra for the assumed site of SPEAR building which is the same as Figure (6).

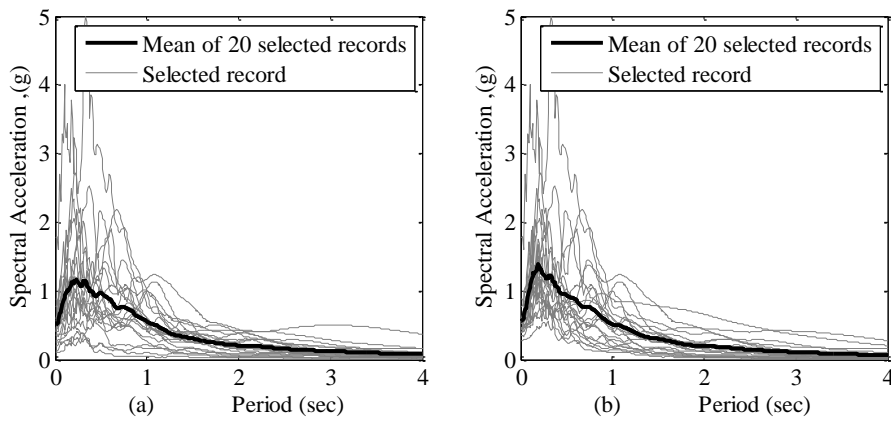


Figure 13: The selected 20 records that their mean matches to the (a) CMS, and (b) E-CMS.

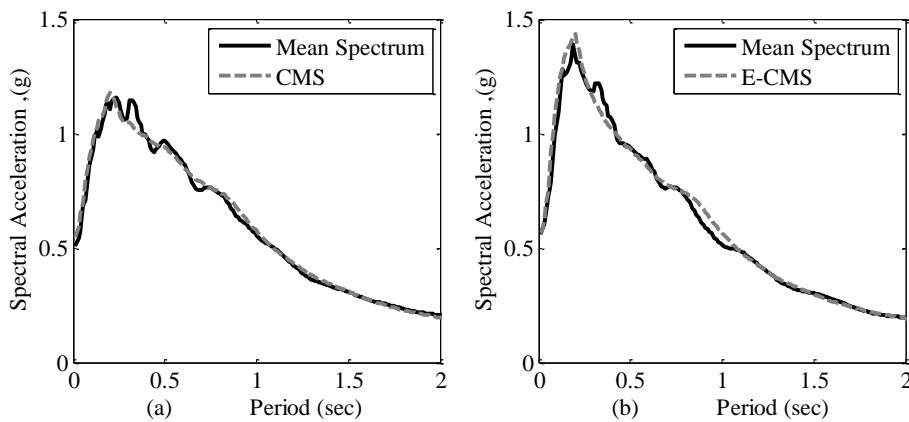


Figure 14: (a) The mean spectrum of 20 selected records and the CMS; (b) The mean spectrum of 20 selected records and the E-CMS.

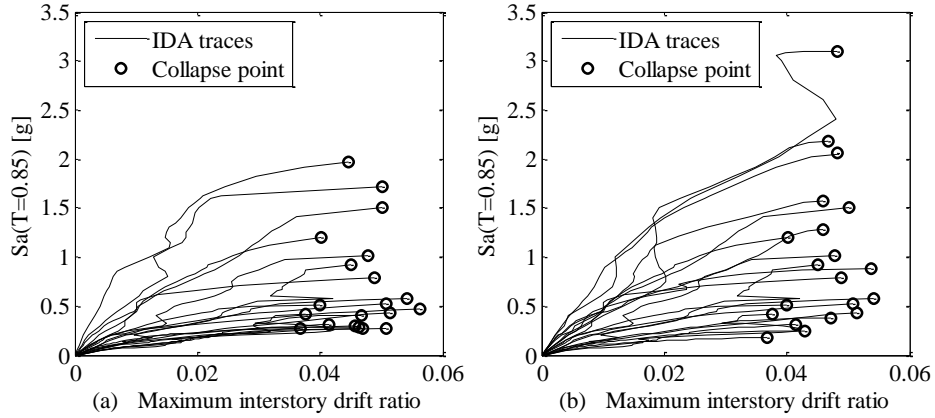


Figure 15: The IDA curves for SPEAR building; (a) based on twenty records which are compatible with CMS; (a) based on 20 records which are compatible with E-CMS.

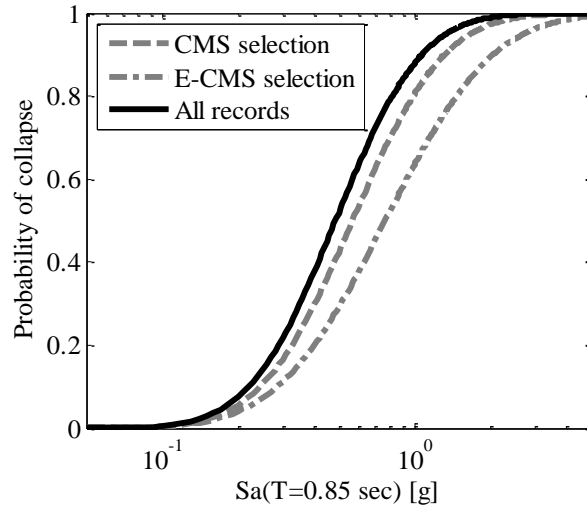


Figure 16: The fragility curves for SPEAR building in 2475 years hazard level.

Table 6: The mean collapse capacity in terms of  $S_a$  for different hazard levels and based on CMS and E-CMS record selection approaches.

Years hazard level	CMS selection	E-CMS selection
475	0.910	0.930
1000	0.851	0.999
2475	0.707	1.003

## 6. CONCLUSIONS

The bias reduction in the estimation of structural response is the main concern of this paper. The performance based earthquake engineering utilizes the intensity measure approach for calculation of the seismic risk. The sufficiency of the employed ground motion intensity measure is always a concern. The problem is that the best ground motion intensity measure is one which has the best correlation with the structural response. Such a ground motion intensity measure can be used without any care to other ground motion characteristics. As the

spectral acceleration is not a perfect ground motion intensity measure, the Epsilon has been introduced to maintain its deficiencies. As seen in Table (5), by employing a wide range of MDOF structures, the Eta parameter is more correlated with the structural response in comparison with the conventional Epsilon. This conclusion had been also observed for SDOF systems in previous researches. Therefore, Eta is a better choice for ground motion selection procedure.

A new emerged target spectrum, named E-CMS, has been investigated in this paper which is based on the Eta indicator. The E-CMS results in reduction of the bias in the estimation of the structural seismic response since the correlation of Eta with the structural response is greater than the correlation between the conventional Epsilon and the structural response. It was shown that the E-CMS amplitude is usually greater than the CMS amplitude, in short period range, which means that the conventional CMS underestimates the structural response in some cases.

The implementation of Epsilon and Eta filtration approaches, and the record selection based on CMS and E-CMS, were also investigated in this paper. The results show that the bias can be decreased by incorporation of the Eta concept into the record selection procedure. This difference is more significant in higher hazard levels and in the case of the structures with low natural periods or with significant higher mode effects. It is worth mentioning that the CB08 GMPE was used throughout the paper for the purpose of consistency. The influence of GMPE on the obtained results can be investigated in future researches. In addition, the considered structures are classified as reinforced concrete frames with regular mesh. The validity of the results for other structures can be investigated in further works e.g. steel buildings, irregular structures, masonry buildings, frames with infill and etc.

## ACKNOWLEDGEMENTS

The authors are very grateful to Curt Haselton for providing us with the numerical models of the structures of Table (5). The authors are also very grateful to three anonymous reviewers for their important and valuable comments which helped to improve the paper.

## REFERENCES

1. FEMA-350, *Recommended seismic design criteria for new steel moment-frame buildings*, 2000: SAC Joint Venture, Federal Emergency Management Agency, Washington, DC.
2. Shome, N. and C.A. Cornell, *Structural seismic demand analysis: consideration of collapse*. Proceedings of the 8th ASCE Specialty Conference on Probabilistic Mechanics and Structural Reliability, 2000. **paper 119, Notre Dame; 1-6**.
3. Baker, J.W. and C.A. Cornell, *Which Spectral Acceleration Are You Using?* Earthquake Spectra, 2006. **22(2)**: p. 293-312.
4. ASCE7-5, *Minimum Design Loads for Buildings and Other Structures*, 2005, American Society of Civil Engineers/Structural Engineering Institute, Reston ,VA.
5. Kramer, S.L., *Geotechnical earthquake engineering*. 1996: Prentice Hall, Upper Saddle River, N.J.
6. Campbell, K.W. and Y. Bozorgnia, *NGA Ground Motion Model for the Geometric Mean Horizontal Component of PGA, PGV, PGD and 5% Damped Linear Elastic Response Spectra for Periods Ranging from 0.01 to 10 s*. Earthquake Spectra, 2008. **24(1)**: p. 139-171.
7. Stewart, J.P., et al., *Representation of Bidirectional Ground Motions for Design Spectra in Building Codes*. Earthquake Spectra, 2011. **27(3)**: p. 927-937.
8. Naeim, F. and M. Lew, *On the Use of Design Spectrum Compatible Time Histories*. Earthquake Spectra, 1995. **11(1)**: p. 111-127.
9. Baker, J.W. and C.A. Cornell, *Spectral shape, epsilon and record selection*. Earthquake Engineering & Structural Dynamics, 2006. **35(9)**: p. 1077-1095.
10. Shome, N., *Probabilistic seismic demand analysis of nonlinear structures*. Ph.D. Dissertation, Department of Civil and Environmental Engineering, Stanford University, Stanford, CA; 320. <http://www.stanford.edu/group/rms/> (accessed 05/31/2006). 1999.

11. Luco, N., *Probabilistic seismic demand analysis, SMRF connection fractures, and near-source effects*. Ph.D. Dissertation, Department of Civil and Environmental Engineering, Stanford University, Stanford, CA; 260pp. <http://www.stanford.edu/group/rms/> (accessed 05/31/2006). 2002.
12. Luco, N. and C.A. Cornell, *Structure-specific scalar intensity measures for near-source and ordinary earthquake ground motions*. *Earthquake Spectra*, 2007. **23**(2): p. 357–392.
13. Tothong, P. and N. Luco, *Probabilistic seismic demand analysis using advanced ground motion intensity measures*. *Earthquake Engineering & Structural Dynamics*, 2007. **36**: p. 1837-1860.
14. Baker, J.W. and C.A. Cornell, *A vector-valued ground motion intensity measure consisting of spectral acceleration and epsilon*. *Earthquake Engineering & Structural Dynamics*, 2005. **34**(10): p. 1193-1217.
15. Baker, J.W., *Conditional Mean Spectrum: Tool for Ground-Motion Selection*. *Journal of Structural Engineering*, 2011. **137**(3): p. 322-331.
16. Mousavi, M., M. Ghafory-Ashtiany, and A. Azarbakht, *A new indicator of elastic spectral shape for the reliable selection of ground motion records*. *Earthquake Engineering & Structural Dynamics*, 2011. **40**(12): p. 1403–1416.
17. Mousavi, M., M. Shahri, and A. Azarbakht, *E-CMS: a new design spectrum for nuclear structures in high levels of seismic hazard*. *Nuclear structures and design*, 2012. **252**: p. 27-33.
18. PEER. *Pacific Earthquake Engineering Research Center, NGA Database, University of California, Berkeley*, accessed 8/3/2012. Available from: <http://peer.berkeley.edu/ngawest/nga>.
19. Baker, J.W., *Vector-valued ground motion intensity measures for probabilistic seismic demand analysis*, 2005: Report #150, John A.Blume Earthquake Engineering Center, Stanford, CA. p. 321.
20. Abrahamson, N.A. and W.J. Silva, *Summary of the Abrahamson & Silva NGA ground motion relations*. *Earthquake Spectra*, 2008. **24**: p. 67-97.
21. Bazzurro, P. and C.A. Cornell, *Disaggregation of seismic hazard*. *Bulletin of the Seismological Society of America*, 1999. **89**(2): p. 501-520.
22. Goldberg, D., *Genetic Algorithms in Search, Optimization, and Machine Learning*. 1989: Addison-Wesley: Reading, MA.
23. Abrahamson, N.A. and W.J. Silva, *Empirical response spectral attenuation relations for shallow crustal earthquakes*. *Seismological Research Letters*, 1997. **68** (1): p. 94-126.
24. Campbell, K.W., *Empirical Near-Source Attenuation Relationships for Horizontal and Vertical Components of Peak Ground Acceleration, Peak Ground Velocity, and Pseudo-Absolute Acceleration Response Spectra*. *Seismological Research Letters*, 1997. **68**(1): p. 154-179.
25. Haselton, C.B., et al., *Accounting for Ground-Motion Spectral Shape Characteristics in Structural Collapse Assessment through an Adjustment for Epsilon*. *Journal of Structural Engineering*, 2011. **137**(3): p. 332-344.
26. Haselton, C.B. and G.G. Deierlein, *Assessing Seismic Collapse Safety of Modern Reinforced Concrete Moment Frame Buildings*, 2006: Technical Report #156, John A.Blume Earthquake Engineering Center, Stanford University, Stanford, CA.
27. Vamvatsikos, D. and C.A. Cornell, *Incremental dynamic analysis*. *Earthquake Engineering & Structural Dynamics*, 2002. **31**(3): p. 491-514.
28. Tso, W.K., T.J. Zhu, and A.C. Heidebrecht, *Engineering implication of ground motion A/V ratio*. *Soil Dynamics and Earthquake Engineering*, 1992. **11**(3): p. 133-144.
29. Sawada, T., et al., *Relation between maximum amplitude ratio and spectral parameters of earthquake ground motion*, in *Proceedings of 10th World Conference of Earthquake Engineering* 1992: Madrid, Spain.
30. USGS. *PSHA disaggregation*. Available from: <https://geohazards.usgs.gov/deaggint/2008/>.
31. Baker, J.W. and C.A. Cornell, *Correlation of Response Spectral Values for Multicomponent Ground Motions*. *Bulletin of the Seismological Society of America*, 2006. **96**(1): p. 215-227.
32. Baker, J.W. and N. Jayaram, *Correlation of spectral acceleration values from NGA ground motion models*. *Earthquake Spectra*, 2008. **24**(1): p. 299-317.
33. Chiou, B.S.J. and R.R. Youngs, *An NGA Model for the Average Horizontal Component of Peak Ground Motion and Response Spectra*. *Earthquake Spectra*, 2008. **24**(1): p. 173-215.
34. Negro, P., et al., *Full-scale testing of a torsionally unbalanced three-storey nonseismic RC frame*, in *Proceedings of the 13th World Conference on Earthquake Engineering* 2004: Vancouver, Canada; 968.
35. Fajfar, P., et al., *Pre- and post-test mathematical modeling of a plan-asymmetric reinforced concrete frame building*. *Earthquake Engineering and Structural Dynamics*, 2006. **35**(11): p. 1359–1379.
36. Banzhaf W, N.P., R. Keller, and F. Francone, *Genetic Programming – An Introduction On the Automatic Evolution of Computer Programs and its Application*, 1998, Heidelberg/San Francisco: dpunkt.verlag /Morgan Kaufmann.

## APPENDIX A

A proposed closed form solution, in order to obtain the correlation coefficient between Eta values, is presented in Equation (a) for the purpose of practical applications. The genetic programming approach [36] was employed to derive (or evaluate) this relationship.

$$\begin{aligned}
 C_1 &= I(T_{\min} + 0.3592) + \cos(1.45 \tan^{-1}(T_{\max}) \times \cos(8.11T_{\max})) \\
 C_2 &= \tan^{-1}\left(\frac{-I \cos(8.94T_{\max})}{3.98}\right) \\
 C_3 &= \cos\left(\cos\left(\frac{I + T_{\min}}{2T_{\max}}\right)\right) - \exp(\cos(T_{\min}) - 4.054) - 0.6114 \\
 C_4 &= \cos\left(\max\left(\frac{I}{T_{\max}}, -T_{\max}\right)\right) \\
 \rho'_{\eta(T),\eta(T^*)} &= \begin{cases} C_1 + C_2 & T_{\max} < 0.3 \ \& \ T_{\min} < 0.15 \\ C_3 + C_4 & \text{Otherwise} \end{cases} \quad (a)
 \end{aligned}$$

where  $T_{\min}$  and  $T_{\max}$  are, respectively, the small and large periods;  $I$  is the difference between two periods which is always negative (or with negative sign). The valid period range in Equation (a) is between 0.01s to 5s. A sample comparison is shown in Figure (A) to compare the proposed relationship with the observed correlation coefficient values.

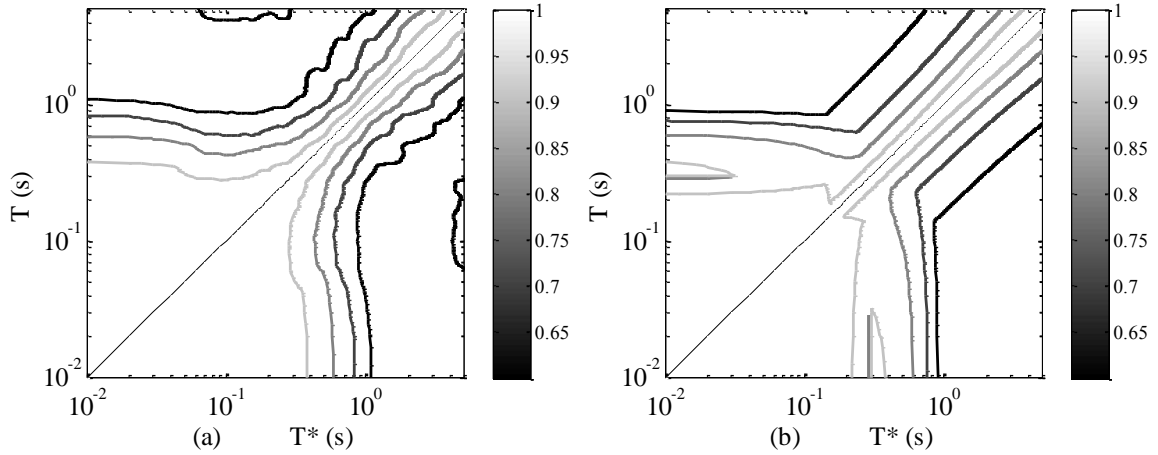


Figure A. a) Correlations from empirical database  
b) Correlations obtained from predictive model.